Interlayer exchange coupling and weakened surface exchange in ultrathin epitaxial Fe(100)/Pd(100)/MgO(100) structures

R. J. Hicken, A. J. R. Ives, D. E. P. Eley, C. Daboo, and J. A. C. Bland
Cavendish Laboratory, University of Cambridge, Madingley Road, Cambridge CB3 0HE, United Kingdom

J. R. Childress and A. Schuhl
Laboratoire Central de Recherches, Thomson-CSF, Domaine de Corbeville, 91404 Orsay, France
(Received 26 October 1993; revised manuscript received 28 April 1994)

Brillouin light scattering (BLS) and the polar magneto-optic Kerr effect (MOKE) have been used to determine the interlayer exchange coupling strength at room temperature in an epitaxial wedge sample of nominal structure Pd/Fe(20 Å)/Pd/Fe(10 Å)/MgO(100) in which the Pd interlayer thickness varied between 14 and 30 Å. The constituent Fe layers were chosen to have different thicknesses and hence possessed different perpendicular anisotropy fields. This allowed both acoustic and optical spin-wave modes to be observed in the BLS experiment and also meant that the polar MOKE experiment could in principle be used to determine both antiferromagnetic and ferromagnetic interlayer coupling strengths. In order that the magnetic parameters of the individual Fe layers be independently determined, superconducting-quantum-interference-device (SQUID) magnetometry, in-plane MOKE, polar MOKE, and BLS measurements have also been made upon reference samples of nominal structure Pd/Fe(20 Å)/Pd(150 Å)/Fe(10 Å)/MgO(100) and Pd/Fe(10 Å)/MgO(100). Comparison of BLS and polar MOKE for the reference samples revealed different values for the effective demagnetizing fields in the two experiments. This is discussed in terms of a possible weakened surface exchange interaction at the Fe/Pd interface. For the wedge structure, ferromagnetic interlayer exchange coupling was observed for the entire range of Pd thicknesses studied.

I. INTRODUCTION

The recent discoveries of antiferromagnetic (AFM) interlayer exchange coupling[1] and a related giant magnetoresistance (GMR) effect[2] in magnetic multilayer films have generated much interest because of the fundamental issues raised and the possible applications in magnetic sensor technology. Since for magnetic recording applications low saturation fields and hence low coupling strengths are desirable, the recent observation by Celinski *et al.* of a weak AFM interlayer exchange coupling in Fe/Pd/Fe/Ag(001) trilayer structures[3] is particularly interesting. It was observed[3] that the coupling was AFM for Pd thicknesses in the range of 13–18 monolayers (ML) while for thinner Pd thicknesses the coupling was ferromagnetic (FM), its magnitude oscillating with a period of 4 ML. The onset of AFM coupling was observed to coincide with a complex lattice reconstruction of the Pd spacer layer, the role of which is unclear, and so it is of interest to determine the nature of the coupling in similar trilayer structures deposited on different substrates for which the detailed growth and structure may differ. Recently Childress *et al.* have explored the magnetic and magnetotransport properties of high-quality epitaxial Fe(100)/Pd(100) superlattices grown upon single-crystal MgO(100) substrates.[4–6] Kerr domain imaging measurements[4] suggested that the coupling was ferromagnetic for the entire range of Pd thicknesses, namely, 10–50 Å, that was studied while the presence of anisotropies was found to complicate the interpretation of *M-H* curves.[5]

The FM coupling strength cannot be determined from in-plane magnetometry measurements unless in-plane anisotropies force the layer magnetizations to depart from parallel alignment. In the present study we have used Brillouin light scattering (BLS) and the polar magneto-optic Kerr effect (MOKE) to directly determine the interlayer exchange coupling strength in an epitaxial Pd(30 Å)/Fe(20 Å)/Pd/Fe(10 Å)/MgO(100) structure (sample *A*) in which the value of the Pd spacer layer thickness varied between 14 and 30 Å. In order to extract FM coupling strengths from either the BLS or polar MOKE experiments, it was necessary to employ Fe layers of different thicknesses,[7] so that the two layers possessed different perpendicular anisotropy fields. Nominal Fe thicknesses of 10 and 20 Å were chosen to this end. In order that the magnetic properties of the two constituent Fe layers be independently checked we have also studied two reference samples with nominal structures: Pd(30 Å)/Fe(10 Å)/MgO (sample B) and Pd(30 Å)/Fe(20 Å)/Pd (150 Å)/(Fe(10 Å)/MgO (sample *C*).

In Sec. II of this paper, we begin by describing the conditions under which the samples were grown and the method of thickness calibration used. In Sec. III we describe the experimental arrangements used in the BLS and polar MOKE studies and the theory used to interpret the BLS data. In Sec. IV, results for samples *B* and *C* are presented and the values of certain quantities deduced from the BLS and polar MOKE experiments are compared. Measurements on sample *A* are presented in Sec. V and the value of using two techniques to determine the FM coupling strength is demonstrated. In Sec. VI, the main results of this work are summarized and discussed.

0163-1829/94/50(9)/6143(8)/$06.00

II. SAMPLE PREPARATION

Growth conditions for the three samples in this study were similar to those for Fe/Pd superlattices, for which extensive structural characterizations have been carried out.[4,5] The samples were grown in a Riber molecular beam epitaxy (MBE) system in which the pressure was 2×10^{-10} Torr during the sample growth. Fe(100) grows on MgO(100) such that the Fe [011] and MgO [001] axes are parallel. Reflection high-energy electron-diffraction (RHEED) patterns from an Fe layer grown directly onto the MgO showed[5] broad streaks characteristic of a nearly two-dimensional growth mode. The RHEED streaks became progressively narrower for subsequent Fe and Pd layers, indicating an improved flatness at the top surface of the sample. Low-angle x-ray diffraction and transmission electron microscopy (TEM) have confirmed the integrity of the layer structure.[5] The TEM measurements showed that the layers were continuous and free of grain boundaries over lateral distances of several thousand Angstroms while the surface roughness was on the order of 5 Å. High-resolution TEM (Ref. 4) revealed excellent coherence between successive atomic planes at both Fe/MgO and Fe/Pd interfaces, again confirming the epitaxial nature of the samples.

It was previously noted[5] that a uniaxial anisotropy, the axis of which was parallel to one of the in-plane cubic axes of the Fe, often appeared in the superlattice samples. Such an anisotropy is not expected for an ideal cubic film of (100) orientation and it was suggested that the origin of this anisotropy lay in the growth geometry since, first, it could be suppressed by rotating the substrate during deposition of the Fe layers, and second, its strength oscillated as a function of the Pd spacer thickness with a period of approximately one monolayer. The consequence of the uniaxial anisotropy was that SQUID magnetometry revealed stepped loops of reduced remanence when the magnetic field was applied parallel to just one of the in-plane Fe cube edges. It was noted that this effect could easily be mistaken for the presence of AFM interlayer coupling if magnetometry measurements were performed for only the easy direction for which the stepped loops occurred. For the samples to be described here, the substrates were always rotated during the growth of the Fe layers and so no significant in-plane uniaxial anisotropy is expected. A wedge-shaped Pd layer was deposited in sample *A* by tilting the substrate away from normal incidence to the Pd flux. The thicknesses of both Fe and Pd layers were determined by operating the Knudsen cells at fixed temperatures, so that the growth rates were fixed (4 Å/min for the Fe and 3 Å/min for the Pd), and then controlling the deposition time. The growth rates were checked by making surface profilometer measurements on specially grown thicker films. Similarly the wedge profile in sample *A* was determined by surface profilometer measurements on a thick Pd film grown at the same substrate tilt angle. The total thicknesses of the completed structures, that is the sums of all of the Fe and Pd layer thicknesses, in samples *B* and *C* were measured by means of low-angle x-ray diffraction and were found to be respectively 7 and 10% less than the stated nominal values.

III. THE BLS AND POLAR MOKE EXPERIMENTS

The BLS measurements were performed in the standard backscattering geometry, with the magnetic field applied perpendicular to the plane of incidence and with an angle of incidence of 45° being used. The sample holder was attached to a rotary mount so that a magnetic field of up to 7 kOe could easily be applied in any direction in the plane of the film with an accuracy of better than one degree. The light source was a single-mode argon-ion laser operating on the 5145-Å line, that provided up to 150 mW of power at the sample. The backscattered light was collected with a $f/\#1.8$ camera lens and analyzed with a Sandercock 3+3 pass tandem Fabry-Perot interferometer[8] before being detected with a photon counting photomultiplier tube. All measurements were made at room temperature.

In order to interpret the BLS measurements we have employed a continuum theory based upon that of Ref. 9 but modified to account for the case of a film of (100) orientation. The effects of both volume and surface anisotropies and also of exchange are taken into account. A similar calculation for single layers was reported by Cochran and Dutcher.[10] For small applied field strengths, canting of the magnetization is taken into account by assuming that the magnetizations either exhibit a coherent rotation or else follow a minimum-energy path.[11] For the case of trilayers, interlayer exchange coupling is also included. A similar theory has been used by Hillebrands[12] to calculate mode frequencies for a number of multilayer systems.

The polar MOKE measurements were performed at room temperature in an Oxford Instruments 70-kOe superconducting magnet, the samples being placed near to the center of the magnet in a reentrant bore tube. This had the advantage that the measurements could be made without the laser beam passing through any window or lens in the vicinity of the magnet field, and so any unwanted Faraday rotation or birefringence in these components was avoided. The beam from a 50-mW HeNe laser, the intensity of which was stabilized to better than 0.1%, was directed on to the sample at near normal incidence. We estimate that the field direction could be aligned parallel to the sample normal with an accuracy of about 1°.

IV. REFERENCE SAMPLES

In-plane longitudinal MOKE measurements were made upon samples *B* and *C* in order to estimate the magnitude of K_1, the first-order cubic magnetocrystalline anisotropy constant. Although the loops were somewhat noisy (the laser used for the longitudinal MOKE measurements was found to be less stable than that used for the polar MOKE measurements), fourfold anisotropies were observed and we estimate the hard axis saturation fields $2K_1/M$ to be approximately 40 Oe for sample *B* and between 50 and 100 Oe for sample *C*. Although these values are much smaller than the value of 525 Oe that is expected for a film with bulk values of K_1 and M, we note that reduced values of $2K_1/M$ that are thickness dependent have been previously reported for ultrathin

Fe(100) films[7,13,14] and that our values are comparable with the smallest of these reported values.[13] MgO cleaves along the ⟨100⟩ directions and so the Fe ⟨110⟩ axes are expected to be parallel to the edge of the substrate. The in-plane MOKE measurements verified that the hard axes were indeed parallel to the substrate edges for sample *B* but for sample *C* the substrate edge was instead found to be an easy axis.

Hysteresis loops obtained by superconducting-quantum-interference-device (SQUID) magnetometry are shown in Fig. 1. The maximum applied field was 10 kOe and the loops were found to vary linearly with applied field above a field value of about 3 kOe. This linear background was fitted and then subtracted. While the SQUID loops saturate at fields of the order of 2 kOe, Kerr domain imaging measurements at a temperature of 300 K have shown[4] that the Fe layer magnetizations reverse by nucleation and propagation of domain walls in much lower fields. We therefore suggest that the large observed saturation fields may be due first to a nonlinear response of the MgO substrate and second to the presence of a moment on the interfacial Pd atoms that is slow to saturate. An additional moment associated with the Fe/Pd interface has been both predicted and observed.[4,13,15,16] Only the low-field parts of the loops are shown in Fig. 1. That the loops are not closed at the maximum field shown may be due either to an instrumental effect or else to hysteresis in the response of the Pd moment. However, we have used the low-field parts of the loops to estimate values for the Fe layer moments in samples *B* and *C*. For sample *B* we take the moment at $T=300$ K to be the extrapolated remnant value since the field was applied along the easy [001] axis and the moment at $T=15$ K to be $\sqrt{2}$ times the remnant value since the field was applied along the hard [011] axis. The coercive field at $T=300$ K was too small to resolve with the magnet used for the SQUID measurements but field-cooled and zero-field-cooled temperature scans revealed no trace of superparamagnetism in sample *B*. The loops for sample *C* are rounded rather than being square as would be expected for an easy axis loop. The loop at $T=300$ K clearly shows that the 10-Å layer reverses before the 20-Å layer. As will be discussed in the next paragraph we believe that in sample *C* the hard [011] axis of the 20-Å layer lies parallel to the easy [001] axis of the 10-Å layer and so the moment at $T=15$ K was measured from the loop at a field of 500 Oe, i.e., at about the hard axis saturation field expected for a bulklike film. At $T=300$ K the total moment was measured at a field value of about 80 Oe which is the saturation field expected from BLS measurements (see the next paragraph). The surface areas of both samples were determined to within 5%. By assuming the bulk value of 1740 emu/cm^3 for the Fe magnetization at $T=15$ K we then deduce total Fe layer thicknesses of 11.0 and 29.7 Å for samples *B* and *C*, respectively, which are close to the nominal values of 10 and 30 Å. The values of the moments at 300 K are smaller than the values at 15 K by 29 and 24% for samples *B* and *C*, respectively. Since definite values will be required later for the analysis of the data, we will assume the nominal values of the layer thicknesses in the three samples that were determined from the flux calibration, and the bulk value of 1710 emu/cm^3 for the room-temperature magnetization of the Fe layers. No additional interfacial moment will be assumed. It is clear that the magnetization is actually reduced from the bulk value at 300 K. The effect of this on our estimate of the interlayer coupling strength will be discussed in Sec. V.

BLS measurements were made upon samples *B* and *C* with the field applied in a number of different directions in the film plane. For sample *B* the frequency variation was too small to be determined accurately while the results for sample *C* are shown in Fig. 2. The fitted curve assumes a value for $2K_1/M$ of 82 Oe. The frequency minimum at 0° in Fig. 2, which corresponds to a hard axis direction, was found to occur when the magnetic field was applied at 45° to the substrate edge, in agreement with the MOKE measurements. For a trilayer

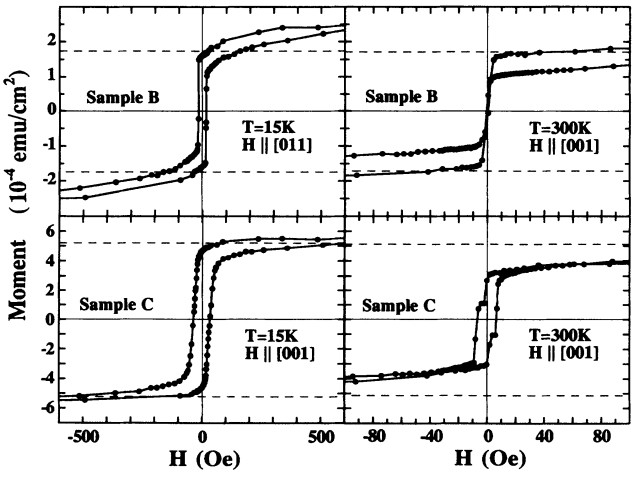

FIG. 1. The moment per unit surface area as determined by SQUID magnetometry is plotted against applied field strength for samples *B* and *C* at $T=15$ and 300 K. The orientation of the applied field relative to the crystallographic axes of the 10-Å Fe layer is indicated in each diagram. The dashed lines indicate the product of the total nominal Fe layer thickness and the bulk value of the Fe magnetization.

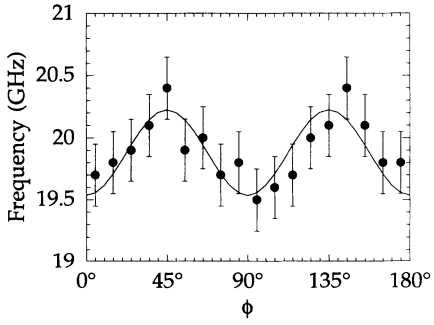

FIG. 2. The BLS mode frequency is plotted as a function of the angle ϕ between the applied magnetic field and one of the in-plane hard axes, for sample *C*. The applied magnetic field strength was 2 kOe for all measurements. The theory curve assumes the parameter values presented in Table I.

structure in which there is no interlayer exchange coupling the surface spin-wave modes of the constituent layers, the so called Damon-Eshbach (DE) modes,[17] are AFM coupled by dipolar interactions across the spacer layer and hence the acoustic spin-wave mode, for which the magnetizations in the two layers precess in phase, lies at a higher frequency than the optical mode, for which the magnetizations precess out of phase.[7] Since the optical fields interfere constructively for the acoustic mode but destructively for the optical mode, the acoustic mode is expected to be the more intense. Therefore, for sample *C*, in which the Pd spacer is sufficiently large as to make any interlayer exchange coupling negligible, the acoustic mode is expected to lie highest. In fact, only one mode was observed which we identify as the acoustic mode. Calculations show that the frequency of this mode is virtually identical to that which would be observed from the thicker Fe layer if it could be measured in isolation from the thinner layer. Therefore, the BLS measurements made upon sample *C* provide information only about the thicker of the two Fe layers. From Fig. 2 we see that this layer possesses the fourfold anisotropy that is characteristic of a Fe(100) layer but we conclude that during the deposition of sample *B* the crystallographic axes of the thicker Fe layer have been rotated through 45° relative to those of the substrate and the thinner Fe layer. It is possible that this surprising observation may be related to a structural transition in the Pd spacer layer although we have no firm evidence to support this explanation.

In Fig. 3, we present the values of the frequency shifts observed when BLS measurements were made with a magnetic field of variable strength applied parallel to the edge of the MgO substrate. If we consider firstly sample *B*, the best-fit curve in Fig. 3 assumes bulklike values of 2.09 for the *g* factor and 2×10^{-6} erg/cm for the exchange, constant *A*, and the value of $2K_1/M$ given above. The effective demagnetizing field, which we define as

$$(4\pi M)_{\text{eff}}=4\pi M-\frac{4K_S}{Md}\ , \tag{1}$$

in which *d* is the layer thickness, *M* is the magnetization, and K_S is the magnetic surface anisotropy constant, was found to have a value of 6.5 kOe. It has been noted previously[7] that it is the effective demagnetizing field rather than the individual values of the constants *M*, *d*, and K_S that determines the position of the observed DE mode. This quantity is also the dominant term in the expression for the saturation field for an *M-H* curve in which the magnetic field is applied normal to the film surface:

$$H_a=(4\pi M)_{\text{eff}}-\frac{2K_1}{M}\ . \tag{2}$$

We have measured H_a by means of polar MOKE, as shown in Fig. 4, and obtain a value of 8.1 kOe that is significantly larger (by 1.6 kOe) than that expected from the BLS measurements. For sample *C*, the best fit to the BLS measurements displayed in Fig. 3 requires an effective demagnetizing field of 17.3 kOe for the 20-Å layer compared to a perpendicular saturation field of 19.7 kOe as measured by polar MOKE. We see that the polar MOKE loop for sample *C*, that is shown in Fig. 4, also exhibits a clear kink at a field of 6.1 kOe at which the thinner Fe layer presumably saturates. The fact that the loop is unrounded and exhibits this sharp kink is clear evidence that the two Fe layers are decoupled in this sample. If we assume the bulk value for the magnetization then the values of the kink and saturation fields imply positive values of the average surface anisotropy constant K_S for both the thick and thin Fe layers. In principle, the height of the kink could also be used to deduce the ratio of moments in the two Fe layers but since there will be a substantial optical skin depth effect for a Pd spacer layer of thickness 150 Å, and since the optical constants of the thin film are not well known, we have not attempted to extract this ratio.

In the BLS experiment the static magnetization lies in the plane of the sample whereas the polar MOKE saturation field determines the point at which the static magnetization just becomes normal to the plane of the sample. Interfacial roughness may induce in-plane demagnetizing fields in both experiments, but these will be averaged on a length scale equal to one laser wavelength (~0.5 μm) in the BLS experiment and to the laser spot diameter (~1 mm) in the MOKE experiment. Both of these length scales are expected to be much longer than that of the atomic scale roughness and so identical average demag-

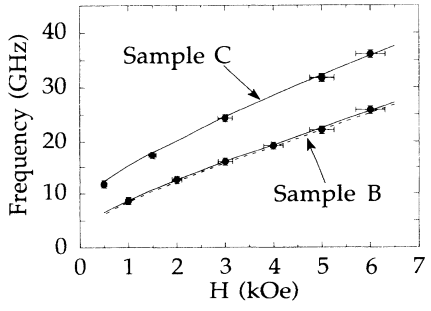

FIG. 3. The BLS mode frequencies of samples *B* and *C* are plotted as a function of the applied field strength, *H*. The field was applied parallel to the edge of the MgO substrate in each case. The calculated curves assume the parameter values presented in Table I. The dashed curve is the expected position of the optical mode for sample *C*.

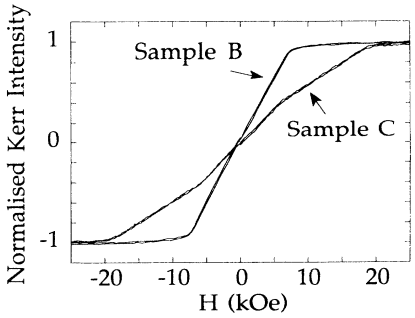

FIG. 4. The normalized Kerr intensity from samples *B* and *C* is plotted as a function of the magnetic field strength *H* for polar MOKE measurements in which the field was applied parallel to the film normal.

netizing factors are expected for the MOKE and BLS experiments. A simple calculation for an oblate ellipsoid of revolution shows that the same combination of out-of-plane and in-plane demagnetizing factors appears in the expressions for both the hard axis saturation field and also the uniform mode ferromagnetic resonance frequency. Interfacial roughness does not therefore provide a trivial explanation of the different demagnetizing fields observed in the two experiments. For a real film, the demagnetizing fields will be nonuniform and then their influence upon our two experiments is more difficult to predict. The discrepancy between the two experiments might also result from an additional fourth-order perpendicular anisotropy. However this would result in a significant curvature in the polar M-H curve in disagreement with our experimental results.

Alternatively we suggest that agreement between the polar MOKE and BLS experiments can be obtained by relaxing the value of the exchange constant at the Fe/Pd interface. Recently O'Handley and Woods[18] have shown that for a surface anisotropy strength less than a critical value (6 ergs/cm^2 in bulk Fe), the magnetization is completely in plane, and that a spatially varying solution only arises when the critical surface anisotropy strength is exceeded. This analysis was originally applied to a semi-infinite magnetic medium, but similar behavior is expected in an ultrathin film. Since in our films the anisotropy strength is at most 0.7 ergs/cm^2 (see Table I), we assume that the uniform solution applies and therefore that the exchange constant does not appear in Eq. (2). However, the dynamical component of the magnetization is nonuniform, and therefore the surface exchange strength affects the DE mode frequency. This can be seen to result from the exchange boundary condition,[19] in which replacing the exchange constant A, with the surface value, A_S, is simply equivalent to rescaling K_S by a factor of A/A_S.

The values of the cubic anisotropy and effective demagnetizing fields obtained from the BLS and MOKE experiments are shown in Table I. The fitted curves in Figs. 2 and 3 assume the values of the anisotropy constants K_1 and K_S that are shown in Table I. The value of K_1 assumed for the MOKE experiment is shown because, as seen from Eq. (2), it enters in the determination of the effective demagnetizing field in the polar MOKE experiment. The expected position of the optical mode for sample C has also been plotted as a dashed line in Fig. 3 and is found to lie close to the acoustic mode position for sample B.

V. WEDGE SAMPLE

In-plane MOKE measurements made upon sample A indicated that the substrate edge was a hard axis and that the saturation field was similar to that for sample C. We shall assume then that the same values for the in-plane anisotropy fields $2K_1/M$ obtained for samples B and C, may be applied to the relevant layers in sample A, except that in sample A the crystallographic axes of the two Fe layers remain parallel. This is not surprising since the Pd interlayer thickness is much smaller in sample A than in sample C.

BLS measurements were made on sample A with the applied magnetic field direction perpendicular to the direction of the gradient in the Pd spacer thickness. The sample was 30 mm long in this latter direction and could be positioned to better than 1 mm by means of a simple translation stage. The Pd spacer thickness could then be determined from the calibration performed on a thicker film grown in an identical geometry. The error in the Pd thickness due to the positioning of the laser spot was less than 1 Å. The frequencies of the modes observed at a point at which the thickness of the Pd spacer was 28 Å are shown in Fig. 5, while spectra for selected data points are shown in Fig. 6. The low-frequency mode can be seen to have the greater intensity for the entire range of field values used, which is a clear signature of FM interlayer coupling. We note also the similarity in the mode positions in Figs. 3 and 5. The acoustic mode frequency in Fig. 5 is determined mainly by the material parameters of the thinner Fe layer in sample A whereas the optical mode position is determined mainly by the material parameters of the thicker Fe layer.

BLS measurements were also made at more than 20 different positions along the wedge profile with an applied magnetic field strength of 3 kOe. The observed mode frequencies have been plotted in Fig. 7(a). It was found that the less intense optical mode was always at a higher frequency than the acoustic mode, and that its intensity rel-

TABLE I. Values of $(4\pi M)_{\text{eff}}$ and $2K_1/M$ are tabulated for the experiments from which they were determined and the values of K_S and K_1 used in the analysis of each experiment are shown. The nominal values of the layer thicknesses and magnetizations are shown. Bulk values of $g=2.09$ for the spectroscopic splitting factor and $A=2\times10^{-6}$ erg/cm for the exchange constant were also assumed.

		Layer 1				Layer 2			
		$d=10$ Å		$M=1710$ emu/cm^3		$d=20$ Å		$M=1710$ emu/cm^3	
Sample	Method	$(4\pi M)_{\text{eff}}$ (kOe)	K_S (erg/cm^2)	$2K_1/M$ (Oe)	K_1 (erg/cm^3)	$(4\pi M)_{\text{eff}}$ (kOe)	K_S (erg/cm^2)	$2K_1/M$ (Oe)	K_1 (erg/cm^3)
A	MOKE & BLS	7.2	0.61		3.4×10^4	16.9	0.39		7.0×10^4
B	MOKE	8.1	0.57	40	3.4×10^4				
	BLS	6.5	0.64		3.4×10^4				
C	MOKE	6.1	0.66		3.4×10^4	19.8	0.15	50–100	7.0×10^4
	BLS		0.66		3.4×10^4	17.3	0.36	82	7.0×10^4

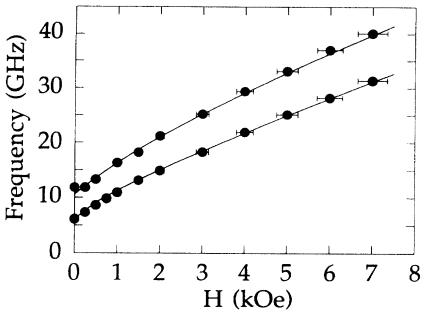

FIG. 5. The acoustic and optical spin wave mode frequencies are plotted as a function of the magnetic field strength H for a point on sample A at which the Pd thickness had a value of 28 Å. The field was applied parallel to the edge of the MgO substrate. The theory curves assume the values of the parameters displayed in Table I and a value of 0.052 erg/cm^2 for A_{12}, the interlayer exchange coupling constant.

ative to the acoustic mode decreased monotonically as the Pd spacer thickness decreased. Indeed for Pd thicknesses less than 21 Å the optical mode became so weak as to be unobservable.

In Fig. 8 are shown perpendicular magnetization curves obtained by polar MOKE for Pd thicknesses of 25.2, 21.6, 19.8, and 17.0 Å. In contrast to the curves in

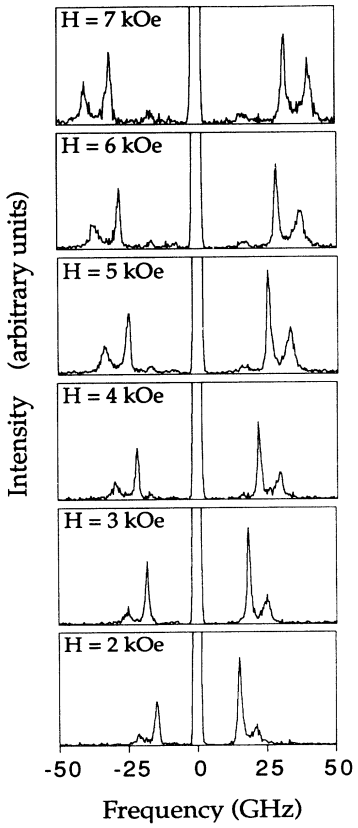

FIG. 6. BLS spectra corresponding to selected data points in Fig. 5 are shown. It can be seen that the more intense acoustic mode always lies at a lower frequency than the less intense optical mode. Arbitrary units have been used for the intensity scale.

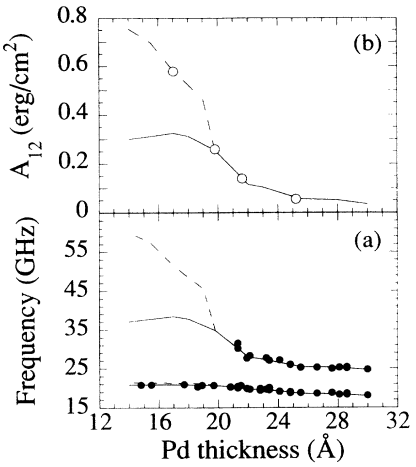

FIG. 7. In (a) the acoustic and optical spin-wave mode frequencies (solid circles) are plotted as a function of the Pd spacer layer thickness for sample A. A magnetic field of strength $H=3$ kOe was applied parallel to the edge of the MgO substrate and perpendicular to the direction of the gradient in the Pd thickness. The solid and dashed theory curves assume the values of the parameters presented in Table I, and values of the coupling constant A_{12} shown in (b). The open circles in (b) indicate the values of A_{12} that were used to generate the fits to the polar MOKE data shown in Fig. 8.

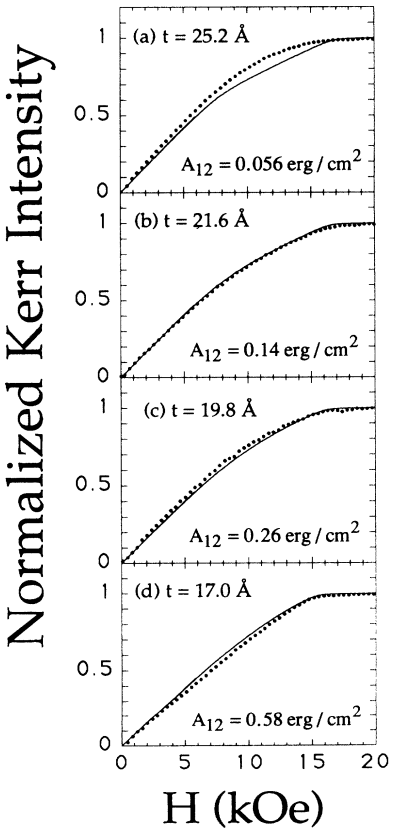

FIG. 8. The normalized Kerr intensity for 4 points on sample A is plotted against the magnetic field strength for polar MOKE measurements in which the magnetic field was applied normal to the film plane. The theory curves assume the values of the parameters presented in Table I. The Pd thicknesses t and the assumed values of the coupling constant A_{12} are indicated in each diagram.

Fig. 4, all four curves in Fig. 8 show significant rounding, again indicating the presence of interlayer coupling. While for the case of zero coupling we expect to obtain a polar MOKE curve similar to that obtained for sample *C*, for a large FM coupling we instead expect to obtain a curve of constant slope that saturates at a field value between that of the kink and saturation fields for the uncoupled loop. Therefore, from Fig. 8 we see that the curves become straighter as the Pd thickness decreases, suggesting that the FM interlayer coupling is becoming increasingly strong.

The BLS and polar MOKE data were fitted simultaneously. It became immediately clear that the best fit parameters for sample *C* were inappropriate for sample *A*, indicating that the Fe layers in the two samples were not exactly identical. Again this is not surprising since RHEED patterns suggest that the thicker Pd spacer in sample *C* leads to a rougher 20-Å Fe layer than in sample *A*. The fit to both experiments depends largely upon three quantities, the effective demagnetizing fields of the two Fe layers and also the interlayer coupling energy per unit area which we shall define to have the form

$$E = -2A_{12}\hat{\mathbf{M}}_1 \cdot \hat{\mathbf{M}}_2 , \tag{3}$$

in which A_{12} is the exchange coupling constant and $\hat{\mathbf{M}}_1$ and $\hat{\mathbf{M}}_2$ are unit vectors in the directions of the magnetizations in the two layers. Again we have assumed the nominal values of 10 and 20 Å for the Fe layer thicknesses, and the bulk value for the Fe magnetization. The average surface anisotropy constants of the two layers, $K_S^{(1)}$ and $K_S^{(2)}$, then remain as variable parameters that determine the effective demagnetizing fields. Saturation fields, H_{sat}, were estimated from the four polar MOKE curves and values of A_{12} were calculated for different combinations of $K_S^{(1)}$ and $K_S^{(2)}$ from the expression

$$A_{12} = \frac{Md_1d_2(H_{\text{sat}} - H_a^{(1)})(H_{\text{sat}} - H_a^{(2)})}{2[d_1H_a^{(1)} + d_2H_a^{(2)} - (d_1 + d_2)H_{\text{sat}}]} , \tag{4}$$

in which d_1 and d_2 are the thicknesses of the two layers and the quantities $H_a^{(i)}$ are as defined in Eq. (2). These parameters were then used to calculate the expected BLS mode frequencies and compared with the experimental data. The best-fit values for the surface anisotropy constants deduced by this method are shown in Table I. Having fixed the values of the surface anisotropy constants the coupling constant A_{12} remains the only variable parameter. The values of A_{12} were then varied again and the values giving the best fit to the BLS measurements are plotted as the solid curve in Fig. 7(b). The shapes of the expected perpendicular magnetization curves have been calculated by means of an energy minimization algorithm that generalizes that of Ref. 11 to the case that the magnetization may move out of the plane of the film. Magnetization curves calculated from the parameter values displayed in Table I and Fig. 7(b) are shown in Figs. 8(a)–8(c). A 0.5° misalignment of the magnetic field direction relative to the film normal has been assumed because the curves do not show the sharp saturation point that is expected for exact alignment of the field. The polar MOKE curves are not true *M-H* curves since optical effects may also be present that are difficult to quantify. However, we see that the calculated and experimental curves are in reasonable agreement. It was found that the polar MOKE curve for a Pd thickness of 17 Å was best fitted by a value of A_{12} of approximately 0.58 erg/cm^2, i.e., a value larger than that obtained by fitting the BLS data. However, for such Pd thicknesses in the region where the optical mode was not observed, the value of A_{12} is not very accurately determined by BLS. To illustrate this point we have used the hypothetical dashed curve in Fig. 7(b) (chosen to include the best estimate of A_{12} obtained from polar MOKE for a Pd thickness of 17Å) to calculate the dashed curves in Fig. 7(a) from which it can be seen that the frequency of the optical mode is much more sensitive to the value of A_{12} than that of the acoustic mode. Hence, in the region where the optical mode is not observed, the value of A_{12} may indeed be larger than that shown by the solid curve in Fig. 7(b). Finally we should remark that the polar MOKE and BLS data could also be fitted by assuming values for the Fe layer thicknesses and magnetizations that were deduced directly from the SQUID data obtained at 15 and 300 K. In this case the dependence of A_{12} on the Pd thickness was similar to that of Fig. 7(b) except that the values of A_{12} were about 16% smaller. The conclusion that the coupling is ferromagnetic for the entire range of Pd thicknesses studied therefore remains unaffected.

VI. CONCLUSIONS

From the studies of samples *B* and *C* we have seen that a static technique (polar MOKE) and a dynamical technique (BLS) may yield somewhat different values for the effective demagnetizing fields in ultrathin Fe/Pd structures. We must stress that this observation does not depend upon the particular values assumed for the thickness, magnetization, and surface anisotropy constants of the relevant layers. We suggested that a weakening of the surface exchange constant at the Fe/Pd interface might resolve this difference. In principle, different spatial variations of the magnetization arise in the static and dynamical cases which result in the surface exchange affecting the value of the effective demagnetizing field determined by BLS, but not the static demagnetizing field determined by polar MOKE. In this model we ignored the presence of moments on the interfacial Pd atoms. However, a more realistic description of this system would include these moments as part of the magnetic layer. Since we would expect the Pd moments to be only loosely exchange coupled to the Fe, this would result in an apparent reduction in the surface exchange of the magnetic layer, Fe plus interfacial Pd layers, as a whole. More detailed modeling of the dynamics of the interface are required to resolve this issue, but we suggest that the combined use of static and dynamical techniques may be a useful method for future investigations of surface exchange interactions.

Good agreement between BLS and polar MOKE was obtained for sample *A* by assuming identical effective

demagnetizing fields in each experiment. We note that the best-fit values of the effective demagnetizing fields for sample *A* are both within 1 kOe of those determined by BLS for samples *B* and *C*. These fields cannot be independently determined for the case of a coupled sample but the success of the fitting procedure suggests that the difference between the static and dynamical values must be relatively small for sample *A*. The main object of this work has been to determine the nature of the interlayer exchange coupling in epitaxial Fe/Pd/Fe trilayers grown upon MgO(100) substrates. Both BLS and polar MOKE experiments unambiguously indicate that the coupling is ferromagnetic for the entire range of Pd thicknesses studied here, although it is of course possible that AFM coupling may exist for larger Pd interlayer thicknesses. The magnitude of the coupling constant A_{12} obtained in this work is larger than that obtained at room temperature in studies of Fe/Pd/Fe trilayer structures grown on Ag(001) crystals.[3] We suggest that this may be due to a greater roughness in our samples since if the coupling strength has a faster than linear dependence on the Pd thickness then a rough Pd spacer layer should produce a larger average coupling strength than a perfectly smooth Pd layer. Finally, the interpretation of either the BLS or polar MOKE experiments is contingent upon a knowledge of a large number of material parameters, and we believe that this study has demonstrated that the combination of two techniques, BLS and polar MOKE, provides a powerful method of reducing the number of variable parameters in the fitting procedure.

[1]P. Grünberg, R. Schreiber, Y. Pang, M. B. Brodsky, and H. Sowers, Phys. Rev. Lett. **57**, 2442 (1986).

[2]M. N. Baibich, J. M. Broto, A. Fert, F. Nguyen Van Dau, F. Petroff, P. Etienne, G. Creuzet, A. Friederich, and J. Chazelas, Phys. Rev. Lett. **61**, 2472 (1988).

[3]Z. Celinski, B. Heinrich, and J. F. Cochran, J. Appl. Phys. **70**, 5870 (1991).

[4]J. R. Childress, R. Kergoat, O. Durand, J.-M. George, P. Galtier, J. Miltat, and A. Schuhl, J. Magn. Magn. Mater. **130**, 13 (1994).

[5]J. R. Childress, A. Schuhl, J.-M. George, O. Durand, P. Galtier, V. Cros, K. Ounadjela, R. Kergoat, and A. Fert, *Magnetism and Structure in Systems of Reduced Dimension,* Proceedings of the 1992 NATO Advanced Workshop in Cargèse, France (Plenum, New York, 1993).

[6]A. Schuhl, J. R. Childress, J.-M. George, P. Galtier, O. Durand, A. Barthelemy, and A. Fert, J. Magn. Magn. Mater. **121**, 275 (1993).

[7]W. B. Muir, J. F. Cochran, J. M. Rudd, B. Heinrich, and Z. Celinski, J. Magn. Magn. Mater. **93**, 229 (1991).

[8]R. Mock, B. Hillebrands, and J. R. Sandercock, J. Phys. E **20**, 656 (1987).

[9]G. T. Rado and R. J. Hicken, J. Appl. Phys. **63**, 3885 (1988).

[10]J. F. Cochran and J. R. Dutcher, J. Appl. Phys. **63**, 3814 (1988).

[11]B. Dieny, J. P. Gavigan, and J. P. Rebouillat, J. Phys. Condens. Matter **2**, 159 (1990); B. Dieny and J. P. Gavigan, J. Phys. Condens. Matter **2**, 187 (1990).

[12]B. Hillebrands, Phys. Rev. B **41**, 530 (1990).

[13]Z. Celinski, B. Heinrich, J. F. Cochran, W. B. Muir, A. S. Arrott, and J. Kirschner, Phys. Rev. Lett. **65**, 1156 (1990).

[14]K. B. Urquhart, B. Heinrich, J. F. Cochran, A. S. Arrott, and K. Myrtle, J. Appl. Phys. **64**, 5334 (1988).

[15]S. Blügel, B. Drittler, R. Zeller, and P. H. Dederichs, Appl. Phys. A **49**, 547 (1989).

[16]J. A. C. Bland, R. D. Bateson, B. Heinrich, Z. Celinski, and H. J. Lauter, J. Magn. Magn. Mater. **104-107**, 1909 (1992); J. A. C. Bland, C. Daboo, B. Heinrich, Z. Celinski, and R. D. Bateson (unpublished).

[17]R. W. Damon and J. R. Eshbach, J. Phys. Chem. Solids **19**, 308 (1961).

[18]R. C. O'Handley and J. P. Woods, Phys. Rev. B **42**, 6568 (1990).

[19]G. T. Rado and J. R. Weertman, J. Phys. Chem. Solids **11**, 315 (1959).